

Capture and Detection of Fentanyl with Thiolated Cucurbit[7]uril Macrocycles on Silver Nanoparticles

Adam S. Braegelman,^{II} Rebekah L. Thimes,^{II} Lindy M. Sherman, Christopher J. Addonizio, Sijie Xian, Maya Lieberman, Jon P. Camden,^{*} and Matthew J. Webber^{*}



Cite This: *ACS Appl. Nano Mater.* 2024, 7, 10879–10885



Read Online

ACCESS |

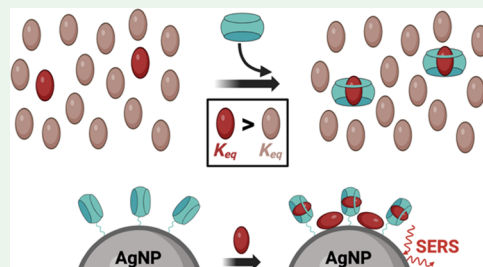
Metrics & More

Article Recommendations

Supporting Information

ABSTRACT: Opioid availability and use have expanded in recent years, leading to a dramatic increase in overdose-related deaths and presenting occupational hazards resulting from exposure to fentanyl and related agents. The high potency of fentanyl is especially concerning given that it is often added to other illicit drugs of abuse in poorly defined quantities; its presence may furthermore be unknown to the user or other individuals encountering the drug substance. Supramolecular macrocycles from the cucurbit[*n*]uril family are known to bind fentanyl and related agents. Here, the selectivity of CB[7] to bind fentanyl in solution is demonstrated by competitive NMR studies with 1 mol % fentanyl in complex drug mixtures of either cocaine or diphenhydramine, which are common cutting agents. A thiolated version of the CB[7] macrocycle is also synthesized for the first time, thereby enabling the direct attachment of CB[7] to the surface of silver nanoparticles (AgNPs). The ability to modify nanoscale colloids with CB[7] has direct application as capture agents in conjunction with the use of AgNPs for surface-enhanced Raman spectroscopy (SERS). When compared to unmodified CB[7], the thiolated CB[7] offers a significant enhancement in fentanyl detection using AgNPs and SERS, with a limit of detection of 0.37 nM. Despite these improvements, nonspecific binding of the fentanyl to the AgNPs surface remains, limiting the specificity and selectivity of fentanyl capture in conjunction with SERS detection. However, the binding selectivity of CB[7] toward fentanyl suggests that it could be leveraged in the design of nanomaterial sensor platforms for the measurement of fentanyl and related compounds in complex mixtures of illicit drugs.

KEYWORDS: supramolecular chemistry, nanotechnology, spectroscopy, opioids, sensors



1. INTRODUCTION

A national emergency surrounds the present epidemic of opioid abuse and overdose in the USA.¹ Among opioid drugs of abuse, fentanyl poses a particular threat due to its potency and ease of illicit manufacture.^{2,3} The addition of small quantities of fentanyl into common drugs, such as cocaine and heroin, is one of the leading causes of opioid overdose and death.^{2,3} Moreover, the exposure to even milligram quantities of fentanyl presents a serious environmental threat to the safety of first responders.^{3,4} Consequently, recent efforts have focused on developing new methods and protocols capable of detecting fentanyl at relevant low concentrations.^{5–10} While technologies exist to reliably detect fentanyl at dilute concentrations, its selective detection and quantification when in complex mixtures of other drug substances present remaining challenges.

Molecular containers of the cucurbit[*n*]uril (CB[*n*]) family have shown promise as synthetic receptors capable of binding drugs of abuse.^{11–13} CB[7] specifically has promise to selectively bind phenethylamine motifs, as found in the molecular structure of fentanyl; CB[7]-fentanyl affinity was reported at $1.8 \times 10^7 \text{ M}^{-1}$.¹³ Unfortunately, due to the extremely high potency of this drug, the binding affinity of

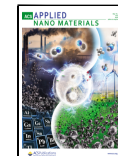
CB[7] is still below the threshold needed to enable sequestration for fentanyl detoxification at lethal drug concentrations occurring in blood,¹⁴ although nascent macrocycles have been reported in recent years that could achieve such affinity.¹⁵ Toward the creation of sensors, CB[*n*] species can be adsorbed to metal surfaces, affording synthetic receptors that sequester small molecule guests of interest near the metal surface; this feature is of particular relevance for surface-specific techniques like surface-enhanced Raman spectroscopy (SERS) using metal nanoparticle sensors.^{16–22} By predictably and selectively sequestering guest molecules near a nanoparticle surface, this approach to detector design has the possibility of significantly enhancing the detection limits of otherwise elusive analytes in complicated matrices. In this work, the selective binding of fentanyl-type drugs to CB[7] is explored via competitive NMR studies on drug mixtures,

Received: March 9, 2024

Revised: April 11, 2024

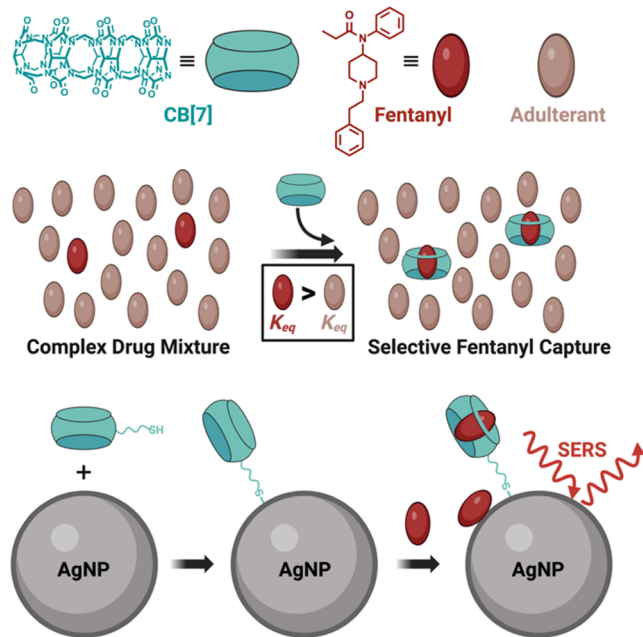
Accepted: April 15, 2024

Published: April 25, 2024



followed by an assessment of the sensing application of a novel thiolated CB[7] macrocycle for anchoring to a silver nanoparticle (AgNPs) substrate for fentanyl detection using SERS (**Scheme 1**). CB[7] is an excellent capture agent for

Scheme 1. Affinity between Cucurbit[7]uril (CB[7]) and Fentanyl for Selective Binding and Detection^a



^aThe affinity between CB[7] and fentanyl enables selective binding in solution, even when the agent is diluted with an adulterant drug (*top*). Endowing CB[7] with a thiol enables covalent display on the surface of silver nanoparticle (AgNPs) colloids for capture and detection of fentanyl using surface-enhanced Raman spectroscopy (SERS), although this method cannot overcome the strong preference for nonspecific fentanyl adsorption to AgNPs (*bottom*).

fentanyl, even in complex drug mixtures, yet SERS assays are complicated by the direct adsorption of fentanyl to the nanoparticle colloid surface.

2. MATERIALS AND METHODS

2.1. CB[7]-SH Synthesis. Monofunctionalized cucurbit[7]uril-butylylchloride (CB[7]-Cl) was synthesized according to previously reported methods.²³ Next, the CB[7]-Cl was combined with 15 equivalents of thiourea in water adjusted to pH 4 using hydrochloric acid. This mixture was stirred for 7 days at 80 °C, with reaction progress monitored using electrospray ionization mass spectrometry (ESI-MS). The reaction was tracked by the evolution of the metastable intermediate, cucurbit[7]uril-thiourea (CB[7]-TU, **Figure S1**). Once CB[7]-TU was observed to be the most abundant species in the reaction mixture, the reaction was adjusted to pH 12 using ammonium hydroxide (NH₄OH) and continued at 80 °C for an additional 1 day. Finally, the reaction mixture was cooled and subsequently precipitated dropwise into methanol, isolating the final cucurbit[7]uril-butanethiol (CB[7]-SH) species. Analysis of the initial and final samples was compared using ¹H NMR (**Figure S2**).

2.2. NMR and Competition NMR. Two adulterants that are typically combined with fentanyl in illicit drug formulations, cocaine and diphenhydramine,^{24,25} were next assessed for CB[7] binding. To assess the binding of CB[7] to each drug, 0.6 mM CB[7] was mixed with 0.75 mM fentanyl, cocaine, or diphenhydramine in D₂O to create a sample of 1:1.25 stoichiometric ratio for ¹H NMR. The preferential binding (i.e., selectivity) of CB[7] to fentanyl over cocaine or diphenhydramine was then evaluated using ¹H NMR. To achieve this,

a series of samples were prepared at fixed concentrations of CB[7] and adulterant, reducing the fentanyl concentration to allow for the direct comparison of competitive binding between species. In this case, 30 mM of either cocaine or diphenhydramine was premixed with 1.5 mM (5%), 0.6 mM (2%), or 0.3 mM (1%) fentanyl in D₂O before adding 4.145 mM CB[7] (all molarities are listed as final sample concentrations). Notably, only the CB[7]-fentanyl interaction yielded peaks within the 6.1–6.6 ppm range, enabling tracking of fentanyl binding. By comparison of the integrals of these shifted (i.e., bound) aromatic fentanyl peaks with the effectively immobile fentanyl methyl peaks at 0.91 ppm, the extent of fentanyl binding to CB[7] was quantified.

2.3. Synthesis of AgNPs. AgNPs were prepared using the Lee and Meisel method.²⁶ Briefly, 90.3 mg of silver nitrate in 530 mL of water was brought to boiling under continuous stirring. Then, 10 mL of 1% (w/v) sodium citrate was added dropwise, and the mixture was boiled with stirring for 20 min. Upon cooling to room temperature, the colloidal dispersion was diluted back up to 500 mL with ultrapure water. Transmission electron microscopy (TEM) analysis of the AgNPs revealed an average particle diameter of 48 ± 8 nm as quantified from multiple TEM images, and UV-vis absorption showed $\lambda_{max} = 405$ nm (**Figure S3**).

2.4. SERS. Samples for the SERS analysis were prepared via a standardized protocol. To 1 mL of AgNPs in water, 150 μ L of 10 μ M CB[7]-SH was added in a volume of 350 μ L of water giving a final concentration of 1 μ M CB[7]-SH in 1.5 mL of total solution volume. This amount of CB[7]-SH was determined through optimization studies (**Figure S4**) to result in surface saturation of the AgNPs. The colloids were then washed several times through centrifugation, removal of 1.4 mL of the supernatant, and redispersion in water. Analytes of interest were then added to the washed CB[7]-modified AgNPs at their stated final concentrations. For the competition experiment between fentanyl and AdNH₂, both analytes were premixed and then added to the washed CB[7]-modified colloids with water to achieve a final volume of 1.5 mL and a final concentration of 1 μ M analytes. The AgNPs were then aggregated using 1 M NaBr. SERS spectra were acquired with a custom-built Raman setup using a 633 nm HeNe laser (Thorlabs). The laser was focused onto the sample using an inverted microscope objective (Nikon, 20 \times , NA = 0.5) with 1 mW power, as measured at the sample. The backscattered radiation was passed through a Rayleigh rejection filter (Semrock) and then dispersed with a spectrometer (Princeton Instruments Acton SP2300, grating = 1200 g/mm). The light was detected using a back-illuminated, deep depletion CCD camera (PIXIS, Spec-10, Princeton Instruments) and recorded using Winspec32 software (Princeton Instruments) with a typical acquisition time of 60 s. All samples were measured in triplicate, for a total of 9 spectra per condition.

3. RESULTS AND DISCUSSION

3.1. CB[7]-Drug Interactions. To investigate the use of CB[7] in the selective binding of fentanyl from complex drug mixtures, the complexation of CB[7] and fentanyl was first verified by ¹H NMR spectroscopy (**Figure 1**). In this sample, CB[7] was mixed with fentanyl at a 1:1.25 stoichiometric ratio of CB[7] to the drug. The binding of fentanyl by CB[7] was observed; notably, proton signals from the phenethylamine ring were shifted upfield from the 7.0–7.4 ppm range to the 6.1–6.6 ppm range upon CB[7] binding. An upfield shift commonly arises for protons located within the cavity of CB[7] in the bound complex as a result of an anisotropic shielding environment in the portal of the macrocycle.²⁷ Importantly, the specific motif that is the key to interaction with CB[7] is conserved across a wide range of fentanyl-like agents, including nascent variants with potency >1000 \times that of fentanyl itself (e.g., carfentanil, 4-methoxymethylfentanyl).

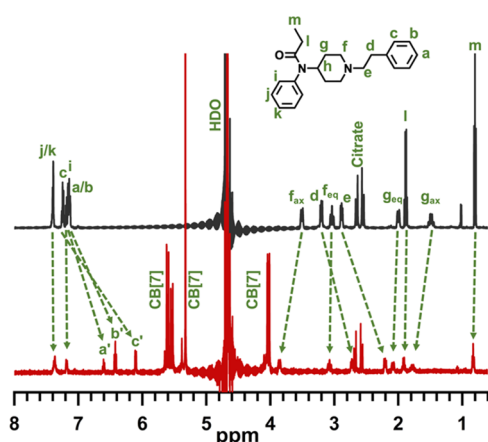


Figure 1. ^1H NMR spectroscopy in D_2O of fentanyl alone (top, black) and fentanyl mixed at a 1:1 ratio with CB[7] (bottom, red). Arrows track peak shifts of fentanyl upon CB[7] binding, with proton labels corresponding to those in the inset structure.

Two common adulterants that are typically combined with fentanyl in illicit drug formulations, cocaine and diphenhydramine,^{24,25} were next assessed for CB[7] binding. Cocaine and diphenhydramine were specifically chosen due to the presence of both aromatics and tertiary amines in both species, similar to the motifs on fentanyl that directly interact with CB[7], and features that are generally predictive of a good guest for CB[7].²⁸ Subsequent ^1H NMR evaluation with samples prepared as above supported some interaction for both cocaine

(Figure S5) and diphenhydramine (Figure S6) with CB[7]; the broadening and slight upfield shift of aromatic signal peaks suggests these to be weak interactions compared to the clear shifts in aromatic peaks of fentanyl upon CB[7] binding. Notably, only the CB[7]–fentanyl interaction resulted in peaks within the 6.1–6.6 ppm range, thereby offering a clear spectroscopic window to monitor CB[7] binding of fentanyl in complex mixtures.

3.2. Selectivity of Fentanyl Binding. The pure component ^1H NMR studies supported the interaction of CB[7] with fentanyl, cocaine, and diphenhydramine. A key requirement of selectively detecting fentanyl within mixtures would be the ability of CB[7] to preferentially bind fentanyl over competing adulterants. Due to its potency and lethality, fentanyl is typically in low abundance relative to other adulterant drugs in these mixtures, further emphasizing the need for good binding selectivity. A series of ^1H NMR samples were prepared at fixed concentrations of CB[7] and adulterant while reducing the fentanyl concentration. In this case, samples were prepared at final concentrations that consisted of 30 mM of either cocaine or diphenhydramine by first mixing with 1.5 mM (5%), 0.6 mM (2%), or 0.3 mM (1%) fentanyl in D_2O before adding 4.145 mM CB[7]. All concentrations are given in terms of their final values in the prepared samples. As is typical with competitive binding experiments, the competing guests were mixed together prior to the introduction of the CB[7], reducing the equilibration time of the competing species in the final solution. Moreover, the adulterant drug was added in large excess to CB[7], increasing the stringency of the

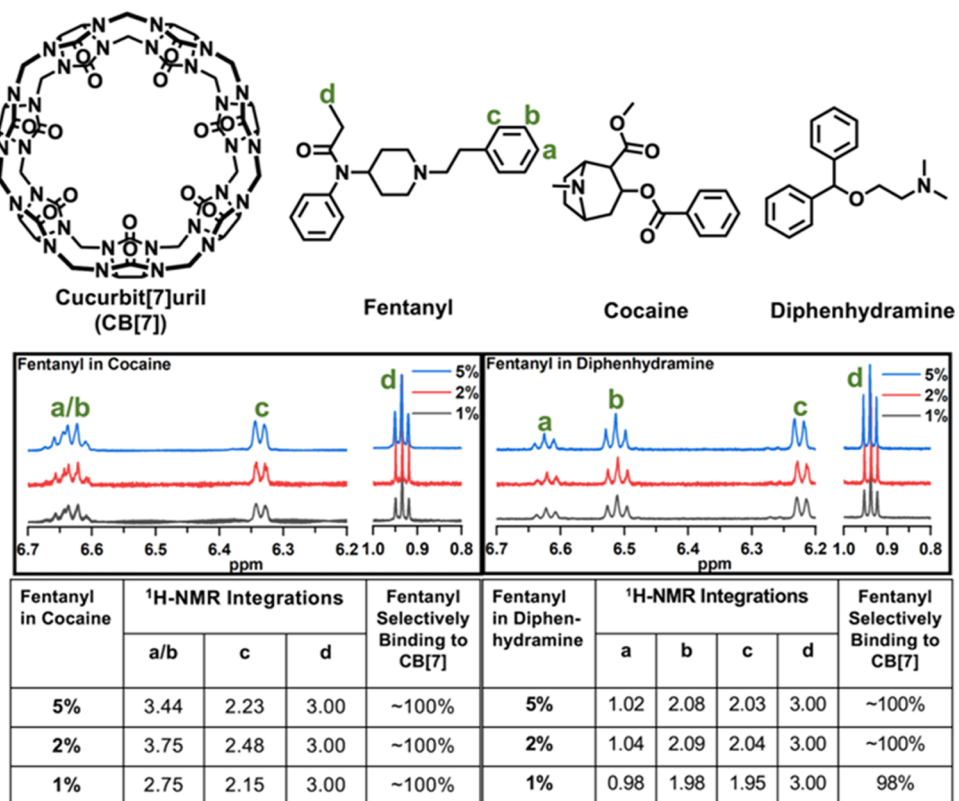


Figure 2. Structure of molecules used (top) to study competition and binding specificity of fentanyl to CB[7] in the presence of cocaine and diphenhydramine. ^1H NMR competition studies for fentanyl mixed at 1, 2, and 5% by mole with cocaine (left) or diphenhydramine (right), tracking shifts in fentanyl protons (a, b, c) due to CB[7] binding relative to immobile fentanyl protons (d). Ratio of shifted protons was used to quantify selective fentanyl capture.

competition. As only the CB[7]–fentanyl interaction yielded peaks within the 6.1–6.6 ppm range, the tracking of fentanyl binding in the mixtures was simplified. By comparing the integrals of these shifted (i.e., bound) aromatic fentanyl peaks with the effectively immobile fentanyl methyl peaks at 0.91 ppm, the extent of fentanyl binding to CB[7] was quantified. Accordingly, these competitive binding experiments revealed a clear preference for the CB[7]–fentanyl interaction in complex drug mixtures (Figures S7 and S8) that was further supported upon quantification (Figure 2). These results confirmed the ability of CB[7] to selectively bind fentanyl in all tested concentrations with near-quantitative (~100%) efficiency on the basis of complete shifting of the specific fentanyl aromatic signals. The binding affinities previously reported for fentanyl ($1.8 \times 10^7 \text{ M}^{-1}$)¹³ compared to that for cocaine ($2.3 \times 10^3 \text{ M}^{-1}$)¹³ or measured here for diphenhydramine ($1.3 \times 10^3 \text{ M}^{-1}$, Figure S9) further support the selectivity reported here for complex mixtures analyzed by ^1H NMR. Accordingly, CB[7] offers promising features supporting its use for selective detection of fentanyl in complex drug mixtures, even in conditions of a high molar excess of a different drug species, resembling the present use of fentanyl coformulated with other drugs of abuse.

3.3. Surface-Reactive CB[7]-SH Variant. To translate the selective binding properties of CB[7] to capture-based detection of fentanyl via SERS, an approach was devised to anchor CB[7] at the surface of silver nanoparticle colloids (AgNPs). Previous reports leveraged the inherent ability of the cucurbituril carbonyl portals to adsorb to metal surfaces by favorable electrostatic interactions.^{16–19} This adsorption mechanism leads to the macrocycle lying flat on the colloid surface or fusing two colloids, sacrificing one or both of the carbonyl portals in the process. This arrangement may thus limit the guest-binding ability of the adsorbed macrocycle. In particular, surface adsorption of the macrocycle may impact its ability to capture larger guests that require threading through both portals of the CB[n] macrocycle. A previous report fully modified a related CB[6] macrocycle at all 12 of its equatorial sites with thiol groups for covalent modification of AgNPs for molecular capture in SERS detection.²⁹ This current work envisioned an alternative approach, appending a short linker bearing a single reactive thiol for the covalent conjugation of CB[7] to AgNPs. Accordingly, a new synthesis of cucurbit[7]-uril-butanethiol (CB[7]-SH) was developed (Figures 3, S1, and S2) that positioned a reactive thiol pendant from an equatorial position on the CB[7] macrocycle. Beginning from a

reported monofunctional cucurbit[7]uril-butyrylchloride (CB[7]-Cl),²³ the chloride was reacted with excess thiourea in pH 4 water at 80 °C for 7 days to generate a cucurbit[7]uril-thiourea (CB[7]-TU, Figure S1). The reaction mixture was adjusted to pH 12 to convert the thiourea intermediate to the free thiol of CB[7]-SH before precipitation in methanol and confirmation via ^1H NMR (Figure 3). An overall yield of 70% CB[7]-SH was achieved by this procedure, determined by integrating protons “D” and “E” relative to “A” as an internal standard. The remainder of CB[7]-Cl was converted to CB[7]-OH in the final base treatment step.

AgNPs were synthesized according to the Lee and Meisel method²⁶ and subsequently characterized by TEM and UV-vis (Figure S3). These AgNPs were surface-saturated with sodium citrate to minimize nanoparticle self-aggregation. This alternate mode of macrocycle attachment to the surface of AgNPs using CB[7]-SH was expected to preserve the ability of CB[7] to sequester larger guests at the colloid surface. UV-vis measurements indicated that the colloids aggregated upon the addition of unmodified CB[7] (Figure S10), evidenced by the loss of the characteristic plasmon signature upon CB[7] addition. However, limited aggregation was observed and a sustained plasmon signature was retained in the CB[7]-SH samples for the duration of the experimentation. This finding is consistent with prior work showing the fusion of colloids through interactions with the portal of the CB[7] macrocycle acting in an adhesive role.¹⁶ Meanwhile, the addition of CB[7]-SH to AgNPs only partially aggregated and destabilized the colloids through the displacement of the citrate layer. These differential outcomes in colloid fusion suggest differences in the orientation of CB[7] when adsorption of the unmodified macrocycle is compared to the covalent attachment of this new thiolated version developed here.

3.4. Integrating CB[7]-SH for SERS. Upon successful synthesis of CB[7]-SH, the ability of this synthetic receptor to enhance analyte detection by SERS on AgNPs was evaluated. AgNPs were exposed to either unmodified CB[7] or CB[7]-SH for 30 min to enable exchange with surface-adsorbed ligands, followed by incubation with analytes for 1 h and subsequent aggregation by sodium bromide. After functionalization with either CB[7] or CB[7]-SH, the SERS-assay potential of CB[7]-modified AgNPs was assessed by detecting 1-adamantanamine (AdNH₂), which is ordinarily silent in SERS. AdNH₂ has a weak affinity for the AgNPs surface that is orders of magnitude weaker than that of more traditional SERS probes. Yet, the high-affinity binding of AdNH₂ with CB[7] (K_{eq} of $4.2 \times 10^{12} \text{ M}^{-1}$)³⁰ makes it an excellent candidate to assess capture-mediated enrichment.

Raman spectroscopy of AdNH₂ at 1 μM in water showed weak signals at 721 and 779 cm^{-1} (Figure 4). Meanwhile, SERS analysis of AdNH₂ alone displayed no quantifiable detection of this analyte. However, when CB[7]-SH was introduced onto the surface of the AgNPs prior to exposure to 1 μM AdNH₂, clear peaks of 721 and 779 cm^{-1} were observable in the SERS spectra. These data suggest that CB[7]-SH can act as a synthetic receptor to sequester the AdNH₂ analyte near the surface of AgNPs, thereby enhancing SERS detection. As AdNH₂ does not need to fully thread the CB[7] macrocycle to achieve its optimal binding position,³⁰ the expected benefits of the alternate orientation of covalently tethered CB[7]-SH are less relevant in this context. Indeed, the capture of AdNH₂ using CB[7]-SH here for SERS detection

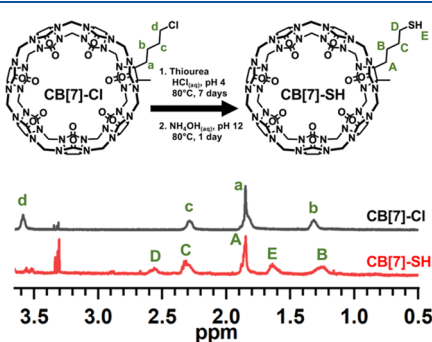


Figure 3. Reaction scheme for the conversion of CB[7]-Cl to CB[7]-SH (top). ^1H NMR in D_2O with labeled peaks of interest, confirming synthesis of the desired product (bottom).

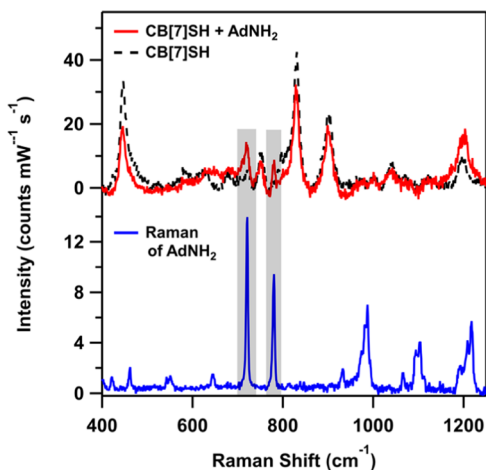


Figure 4. Raman spectra of AdNH_2 powder (bottom) and SERS of $\text{CB}[7]\text{-SH}$ (top, black dashed trace) and $\text{CB}[7]\text{-SH} + 1 \mu\text{M AdNH}_2$ (top, red trace) on AgNPs. The appearance of characteristic AdNH_2 peaks at ~ 720 and 780 cm^{-1} in the red trace support $\text{CB}[7]\text{-SH}$ binding AdNH_2 close to the AgNP surface.

was comparable to that from a prior report using unmodified $\text{CB}[7]$.²²

3.5. Enhancing Fentanyl Limit of Detection. Next, the capture of fentanyl by $\text{CB}[7]$ and $\text{CB}[7]\text{-SH}$ was evaluated to translate the binding observed in ^1H NMR analysis to SERS detection. First, SERS of fentanyl on pristine AgNPs was performed where a characteristic fentanyl peak of 1002 cm^{-1} was observed (Figure S11). Limit of detection (LOD) studies were then performed using AgNPs surface-functionalized with either $\text{CB}[7]$ or $\text{CB}[7]\text{-SH}$ and exposed to varying concentrations of fentanyl. With this experimental design, the LOD is inversely correlated to the signal attenuation of the fentanyl characteristic peak as the fentanyl concentration decreases. When AgNPs were modified with adsorbed $\text{CB}[7]$, the fentanyl signal at 1002 cm^{-1} reduced quickly as fentanyl concentration was decreased, with this characteristic signal being indistinguishable at fentanyl concentrations below 0.5 nM (Figure 5). This result still compares favorably to a

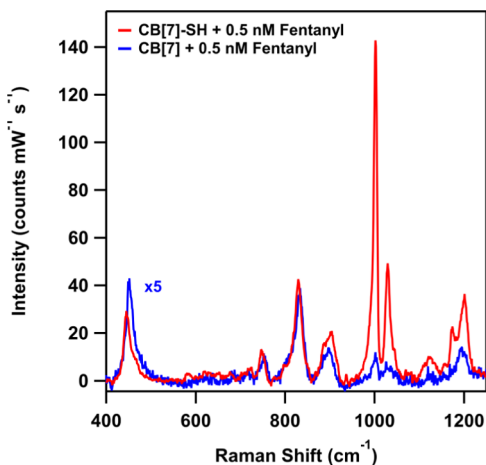


Figure 5. SERS of $\text{CB}[7] + 0.5 \text{ nM fentanyl}$ (blue trace) and $\text{CB}[7]\text{-SH} + 0.5 \text{ nM fentanyl}$ (red trace) on AgNPs. The characteristic peak for fentanyl at $\sim 1002 \text{ cm}^{-1}$ is highly prevalent when $\text{CB}[7]\text{-SH}$ is present but limited when $\text{CB}[7]$ is present. $\text{CB}[7]$ trace (blue) is displayed at $5\times$ its actual signal for ease in visualization.

previously published report performing SERS on AgNPs, in which the fentanyl limit of detection was estimated to be $\sim 14.8 \text{ nM}$.³¹ However, when AgNPs were instead functionalized with $\text{CB}[7]\text{-SH}$, the characteristic fentanyl peak at 1002 cm^{-1} remained the dominant peak in the SERS spectra for a fentanyl concentration of at least 0.5 nM (Figure 5). The limit of detection for $\text{CB}[7]\text{-SH}$ was calculated to be 0.37 nM (Figure S12), a dramatic improvement over the value of $\sim 14.8 \text{ nM}$ that has previously been reported for the detection of fentanyl by SERS on AgNPs.³¹ The limits of detection using SERS on AgNPs with or without $\text{CB}[7]$ -based capture are an improvement over antibody-based lateral flow assays, which can detect fentanyl down to 20 ng/mL ($\sim 59 \text{ nM}$) but are susceptible to false positives from other drugs of abuse.³² These results also support a difference in fentanyl detection sensitivity between AgNPs functionalized with $\text{CB}[7]$ vs $\text{CB}[7]\text{-SH}$, with the latter having an improved LOD for fentanyl. It can be inferred that this difference in sensitivity arises from a difference in the orientation or mode of presentation of the $\text{CB}[7]\text{-SH}$ on the AgNPs surface, especially given the larger size of the fentanyl guest and its likely binding position within the $\text{CB}[7]$ portal evident by proton shifts in ^1H NMR studies (Figure 1). These initial observations thus support a hypothesis that surface-adsorbed $\text{CB}[7]$ is more limited in its ability to bind guests due to one carbonyl portal lying flat on the colloid surface, whereas the covalent attachment of $\text{CB}[7]\text{-SH}$ through its equatorial side chain preserves access to both sides of the macrocycle.

3.6. Limitations from Nonspecific Fentanyl Binding.

Additional experiments were performed to assess if enhanced fentanyl detection is due specifically to fentanyl bound by $\text{CB}[7]\text{-SH}$. Nanoparticles with $\text{CB}[7]\text{-SH}$ were exposed to $1 \mu\text{M}$ fentanyl and $1 \mu\text{M AdNH}_2$ simultaneously, selected to be 1:1:1 by mole with the $\text{CB}[7]\text{-SH}$ on the colloid surface. With fentanyl reported to bind to $\text{CB}[7]$ with an affinity (K_{eq}) of $1.8 \times 10^7 \text{ M}^{-1}$,¹³ and AdNH_2 binding $\text{CB}[7]$ with a reported K_{eq} of $4.2 \times 10^{12} \text{ M}^{-1}$,³⁰ the AdNH_2 would be expected to out-compete fentanyl within the $\text{CB}[7]$ portal at equimolar concentrations. Thus, if fentanyl was detected only on the AgNPs surface through its binding to $\text{CB}[7]\text{-SH}$, then the introduction of AdNH_2 into the analyte mixture should significantly reduce the characteristic fentanyl 1002 cm^{-1} peak. This same effect was observed previously when using AdNH_2 to block $\text{CB}[7]$ capture-based SERS detection of phenylalanine-terminated peptides, with the higher affinity guest successfully preventing SERS detection.²² Unfortunately, this was not observed (Figure S13). When fentanyl and AdNH_2 were simultaneously introduced to AgNPs modified with $\text{CB}[7]\text{-SH}$, the fentanyl 1002 cm^{-1} peak and the AdNH_2 779 cm^{-1} peak were both present in the resultant spectrum. These results indicate that fentanyl is likely interacting with the AgNPs surface through at least one alternative route beyond being bound to the $\text{CB}[7]\text{-SH}$ portal. As fentanyl is known to be both very surface active and highly visible by SERS, including on bare colloids,³¹ even low-level incorporation in the course of AgNP aggregation may be expected to yield nonspecific signal by a $\text{CB}[7]$ -independent mechanism. In LOD studies, the fentanyl signal was saturated at concentrations of $\sim 10 \text{ nM}$ (Figure S12); accordingly adsorption of $<1\%$ of fentanyl added in these studies may still yield a significant signal. Further evaluation also revealed a substantial SERS signal for fentanyl alone on bare AgNPs, even at concentrations of 0.5 nM (Figure S14). This finding represents

a notable improvement over previously published work that showed an LOD of \sim 14.8 nM for the detection of fentanyl by SERS on AgNPs.³¹ Several surface-blocking strategies were employed to mitigate surface-binding in order to probe selective capture using CB[7]-modified surfaces, but none were found that could eliminate nonspecific fentanyl binding without displacing the CB[7]-SH macrocycle. Accordingly, while CB[7]-SH modification offers capture-mediated enhancement in detecting surface-silent guests like AdNH₂, its utility for the detection of highly surface-active analytes like fentanyl remains limited.

4. CONCLUSIONS

The increased prevalence of opioids presents a significant risk of lethal overdose for drug users, many of whom unknowingly consume drugs laced with poorly defined quantities of fentanyl. First responders and military personnel likewise encounter occupational risks from fentanyl in drug products or as a chemical agent. Herein, the CB[7] macrocycle is shown to afford selectivity in binding fentanyl, even at only 1 mol % in a complex mixture with adulterants of illicit drugs cocaine and diphenhydramine. In order to expand the use of CB[7] capture into a sensor platform, a novel CB[7]-SH variant was developed for covalent integration of silver nanoparticle colloids in conjunction with SERS detection. An improvement in the limit of detection was evident for covalent presentation of CB[7]-SH on the AgNPs substrate relative to adsorbed CB[7] or fentanyl alone, enabling clear detection of fentanyl down to at least 0.5 nM. However, the highly surface-active nature of fentanyl on AgNPs limits the utility of its selective capture on the surface of these nanoscale colloids for integration with SERS; when all CB[7] portals should be blocked by a model AdNH₂ adulterant with much higher binding affinity, fentanyl SERS signatures were still clearly evident indicating a preference for adsorption to the AgNPs surface on its own.

■ ASSOCIATED CONTENT

SI Supporting Information

The Supporting Information is available free of charge at <https://pubs.acs.org/doi/10.1021/acsanm.4c01444>.

Reaction schemes; nanomaterial characterization; ¹H NMR; ITC; supporting SERS data; UV/vis absorbance (PDF)

■ AUTHOR INFORMATION

Corresponding Authors

Jon P. Camden — Department of Chemistry & Biochemistry, University of Notre Dame, Notre Dame, Indiana 46556, United States;  orcid.org/0000-0002-6179-2692; Email: jcamden3@nd.edu

Matthew J. Webber — Department of Chemical & Biomolecular Engineering, University of Notre Dame, Notre Dame, Indiana 46556, United States;  orcid.org/0003-3111-6228; Email: mwebber@nd.edu

Authors

Adam S. Braegelman — Department of Chemical & Biomolecular Engineering, University of Notre Dame, Notre Dame, Indiana 46556, United States; Bioengineering Graduate Program, University of Notre Dame, Notre Dame, Indiana 46556, United States

Rebekah L. Thimes — Department of Chemistry & Biochemistry, University of Notre Dame, Notre Dame, Indiana 46556, United States;  orcid.org/0000-0001-6333-126X

Lindy M. Sherman — Department of Chemistry & Biochemistry, University of Notre Dame, Notre Dame, Indiana 46556, United States;  orcid.org/0000-0003-2435-8886

Christopher J. Addonizio — Department of Chemical & Biomolecular Engineering, University of Notre Dame, Notre Dame, Indiana 46556, United States

Sijie Xian — Department of Chemical & Biomolecular Engineering, University of Notre Dame, Notre Dame, Indiana 46556, United States

Marya Lieberman — Department of Chemistry & Biochemistry, University of Notre Dame, Notre Dame, Indiana 46556, United States;  orcid.org/0000-0003-3968-8044

Complete contact information is available at: <https://pubs.acs.org/10.1021/acsanm.4c01444>

Author Contributions

[¶]A.S.B. and R.L.T. contributed equally to this work.

Notes

The authors declare no competing financial interest.

■ ACKNOWLEDGMENTS

This work was supported by the National Institutes of Health under grant R35GM137987 (M.J.W.), the National Science Foundation under Grant CHE-2108330 (R.L.T. and J.P.C.), and a Notre Dame Nanoscience and Technology (NDNano) Seed Grant (M.J.W. and J.P.C.). Any opinions, findings, and conclusions expressed in this material are those of the authors and do not necessarily reflect the views of the National Science Foundation. The authors thank Shayanta Chowdhury for transmission electron microscopy (TEM) measurements and the Notre Dame Integrated Imaging Facility for the use of the Spectra300 TEM.

■ REFERENCES

- (1) McCarthy, M. US Declares Opioid Epidemic a “National Emergency. *BMJ* **2017**, *358*, j3881.
- (2) Armenian, P.; Vo, K. T.; Barr-Walker, J.; Lynch, K. L. Fentanyl, Fentanyl Analogs and Novel Synthetic Opioids: A Comprehensive Review. *Neuropharmacology* **2018**, *134*, 121–132.
- (3) Jannetto, P. J.; Helander, A.; Garg, U.; Janis, G. C.; Goldberger, B.; Ketha, H. The Fentanyl Epidemic and Evolution of Fentanyl Analogs in the United States and the European Union. *Clin. Chem.* **2019**, *65* (2), 242–253.
- (4) Howard, J.; Hornsby-Myers, J. Fentanyl and the Safety of First Responders: Science and Recommendations. *Am. J. Ind. Med.* **2018**, *61*, 633–639, DOI: [10.1002/ajim.22874](https://doi.org/10.1002/ajim.22874).
- (5) Haddad, A.; Comanescu, M. A.; Green, O.; Kubic, T. A.; Lombardi, J. R. Detection and Quantitation of Trace Fentanyl in Heroin by Surface-Enhanced Raman Spectroscopy. *Anal. Chem.* **2018**, *90* (21), 12678–12685.
- (6) Rab, E.; Flanagan, R. J.; Hudson, S. Detection of Fentanyl and Fentanyl Analogs in Biological Samples Using Liquid Chromatography-High Resolution Mass Spectrometry. *Forensic Sci. Int.* **2019**, *300*, 13–18, DOI: [10.1016/j.forsciint.2019.04.008](https://doi.org/10.1016/j.forsciint.2019.04.008).
- (7) Green, T. C.; Park, J. N.; Gilbert, M.; McKenzie, M.; Struth, E.; Lucas, R.; Clarke, W.; Sherman, S. G. An Assessment of the Limits of Detection, Sensitivity and Specificity of Three Devices for Public

Health-Based Drug Checking of Fentanyl in Street-Acquired Samples. *Int. J. Drug Policy* **2020**, *77*, No. 102661.

(8) Barfidokht, A.; Mishra, R. K.; Seenivasan, R.; Liu, S.; Hubble, L. J.; Wang, J.; Hall, D. A. Wearable Electrochemical Glove-Based Sensor for Rapid and on-Site Detection of Fentanyl. *Sens. Actuators, B* **2019**, *296*, 126422 DOI: [10.1016/j.snb.2019.04.053](https://doi.org/10.1016/j.snb.2019.04.053).

(9) Glasscott, M. W.; Vannoy, K. J.; Ashvin Iresh Fernando, P.; Kosgei, G. K.; Moores, L. C.; Dick, J. E. Electrochemical Sensors for the Detection of Fentanyl and Its Analogs: Foundations and Recent Advances. *TrAC, Trends Anal. Chem.* **2020**, *132*, No. 116037, DOI: [10.1016/j.trac.2020.116037](https://doi.org/10.1016/j.trac.2020.116037).

(10) Wilson, N. G.; Raveendran, J.; Docolis, A. Portable Identification of Fentanyl Analogs in Drugs Using Surface-Enhanced Raman Scattering. *Sens. Actuators, B* **2021**, *330*, No. 129303, DOI: [10.1016/j.snb.2020.129303](https://doi.org/10.1016/j.snb.2020.129303).

(11) Shcherbakova, E. G.; Zhang, B.; Gozem, S.; Minami, T.; Zavalij, P. Y.; Pushina, M.; Isaacs, L. D.; Anzenbacher, P., Jr. Supramolecular Sensors for Opiates and Their Metabolites. *J. Am. Chem. Soc.* **2017**, *139* (42), 14954–14960.

(12) Brockett, A. T.; Deng, C.; Shuster, M.; Perera, S.; DiMaggio, D.; Cheng, M.; Murkli, S.; Briken, V.; Roesch, M. R.; Isaacs, L. In Vitro and In Vivo Sequestration of Methamphetamine by a Sulfated Acyclic CB[n]-Type Receptor. *Chem. - Eur. J.* **2021**, *27* (69), 17476–17486, DOI: [10.1002/chem.202102919](https://doi.org/10.1002/chem.202102919).

(13) Ganapati, S.; Grabitz, S. D.; Murkli, S.; Scheffenbichler, F.; Rudolph, M. I.; Zavalij, P. Y.; Eikermann, M.; Isaacs, L. Molecular Containers Bind Drugs of Abuse in Vitro and Reverse the Hyperlocomotive Effect of Methamphetamine in Rats. *ChemBioChem* **2017**, *18* (16), 1583–1588.

(14) Addonizio, C. J.; Gates, B. D.; Webber, M. J. Supramolecular “Click Chemistry” for Targeting in the Body. *Bioconjugate Chem.* **2021**, *32* (9), 1935–1946.

(15) Brockett, A. T.; Xue, W.; King, D.; Deng, C.-L.; Zhai, C.; Shuster, M.; Rastogi, S.; Briken, V.; Roesch, M. R.; Isaacs, L. Pillar[6]MaxQ: A Potent Supramolecular Host for Sequestration of Methamphetamine and Fentanyl. *Chem* **2023**, *9* (4), 881–900.

(16) Sigle, D. O.; Kasera, S.; Herrmann, L. O.; Palma, A.; de Nijs, B.; Benz, F.; Mahajan, S.; Baumberg, J. J.; Scherman, O. A. Observing Single Molecules Complexing with Cucurbit[7]uril through Nanogap Surface-Enhanced Raman Spectroscopy. *J. Phys. Chem. Lett.* **2016**, *7* (4), 704–710.

(17) Chen, G.-Y.; Sun, Y.-B.; Shi, P.-C.; Liu, T.; Li, Z.-H.; Luo, S.-H.; Wang, X.-C.; Cao, X.-Y.; Ren, B.; Liu, G.-K.; Yang, L.-L.; Tian, Z.-Q. Revealing Unconventional Host-Guest Complexation at Nanostructured Interface by Surface-Enhanced Raman Spectroscopy. *Light: Sci. Appl.* **2021**, *10* (1), 85.

(18) Shi, X.; Gu, W.; Zhang, C.; Zhao, L.; Li, L.; Peng, W.; Xian, Y. Construction of a Graphene/Au-Nanoparticles/Cucurbit[7]uril-Based Sensor for Pb(2+) Sensing. *Chem. - Eur. J.* **2016**, *22* (16), 5643–5648, DOI: [10.1002/chem.201505034](https://doi.org/10.1002/chem.201505034).

(19) Chio, W.-I. K.; Moorthy, S.; Perumal, J.; Dinish, U. S.; Parkin, I. P.; Olivo, M.; Lee, T.-C. Dual-Triggered Nanoaggregates of cucurbit[7]uril and Gold Nanoparticles for Multi-Spectroscopic Quantification of Creatinine in Urinalysis. *J. Mater. Chem. C* **2020**, *8*, 7051–7058.

(20) Lv, Y.; Tao, C.-A.; Huang, J.; Li, Y.; Wang, F.; Cai, F.; Wang, J. Self-Assembly of cucurbit[7]uril on the Surface of Graphene/gold Modified Electrode. *Nanomater. Nanotechnol.* **2016**, *6*, No. 184798041668244.

(21) Neirynck, P.; Brinkmann, J.; An, Q.; van der Schaft, D. W. J.; Milroy, L.-G.; Jonkheijm, P.; Brunsved, L. Supramolecular Control of Cell Adhesion via Ferrocene-cucurbit[7]uril Host-Guest Binding on Gold Surfaces. *Chem. Commun.* **2013**, *49* (35), 3679–3681.

(22) Olson, J. E.; Braegelman, A. S.; Zou, L.; Webber, M. J.; Camden, J. P. Capture of Phenylalanine and Phenylalanine-Terminated Peptides Using a Supramolecular Macrocycle for Surface-Enhanced Raman Scattering Detection. *Appl. Spectrosc.* **2020**, *74* (11), 1374–1383.

(23) Vinciguerra, B.; Cao, L.; Cannon, J. R.; Zavalij, P. Y.; Fenselau, C.; Isaacs, L. Synthesis and Self-Assembly Processes of Mono-functionalized cucurbit[7]uril. *J. Am. Chem. Soc.* **2012**, *134* (31), 13133–13140.

(24) Singh, V. M.; Browne, T.; Montgomery, J. The Emerging Role of Toxic Adulterants in Street Drugs in the US Illicit Opioid Crisis. *Public Health Rep.* **2020**, *135* (1), 6–10.

(25) Krauss, S. T.; Ross, D.; Forbes, T. P. Separation and Detection of Trace Fentanyl from Complex Mixtures Using Gradient Elution Moving Boundary Electrophoresis. *Anal. Chem.* **2019**, *91* (20), 13014–13021.

(26) Lee, P. C.; Meisel, D. Adsorption and Surface-Enhanced Raman of Dyes on Silver and Gold Sols. *J. Phys. Chem. A* **1982**, *86* (17), 3391–3395.

(27) Sigwalt, D.; Šekutor, M.; Cao, L.; Zavalij, P. Y.; Hostaš, J.; Ajani, H.; Hobza, P.; Mlinarić-Majerski, K.; Glaser, R.; Isaacs, L. Unraveling the Structure-Affinity Relationship between Cucurbit[n]-urils (n = 7, 8) and Cationic Diamondoids. *J. Am. Chem. Soc.* **2017**, *139* (8), 3249–3258.

(28) Barrow, S. J.; Kasera, S.; Rowland, M. J.; del Barrio, J.; Scherman, O. A. Cucurbituril-Based Molecular Recognition. *Chem. Rev.* **2015**, *115*, 12320–12406.

(29) Kim, N. H.; Hwang, W.; Baek, K.; Rohman, M. R.; Kim, J.; Kim, H. W.; Mun, J.; Lee, S. Y.; Yun, G.; Murray, J.; Ha, J. W.; Rho, J.; Moskovits, M.; Kim, K. Smart SERS Hot Spots: Single Molecules Can Be Positioned in a Plasmonic Nanojunction Using Host–Guest Chemistry. *J. Am. Chem. Soc.* **2018**, *140* (13), 4705–4711.

(30) Liu, S.; Ruspic, C.; Mukhopadhyay, P.; Chakrabarti, S.; Zavalij, P. Y.; Isaacs, L. The Cucurbit[n]uril Family: Prime Components for Self-Sorting Systems. *J. Am. Chem. Soc.* **2005**, *127* (45), 15959–15967.

(31) Wang, H.; Xue, Z.; Wu, Y.; Gilmore, J.; Wang, L.; Fabris, L. Rapid SERS Quantification of Trace Fentanyl Laced in Recreational Drugs with a Portable Raman Module. *Anal. Chem.* **2021**, *93* (27), 9373–9382.

(32) Lockwood, T.-L.; Vervoordt, A.; Lieberman, M. High Concentrations of Illicit Stimulants and Cutting Agents Cause False Positives on Fentanyl Test Strips. *Harm Reduct. J.* **2021**, *18* (1), 30 DOI: [10.1186/s12954-021-00478-4](https://doi.org/10.1186/s12954-021-00478-4).